

Dynamic Characteristic Prediction of Large Satellite Antennas by Component Tests

Masayoshi Misawa*

Shizuoka University, Shizuoka 432-8561, Japan

and

Kenichi Funamoto†

Sansei Yusoki Company, Osaka 564-0063, Japan

The purpose of this study is to predict accurate frequencies of large space structures from component modal test results. We deal with structures such as large satellite antennas, on which it is difficult to perform modal tests on the whole structure. A method, considering the effect of untested components as boundary mass and stiffness, is proposed for obtaining accurate frequencies of a structure. Boundary mass and stiffness are found by reducing mass and stiffness matrices of untested components to boundary degrees of freedom. A tested component with these reduced matrices at the boundary gives accurate frequencies of the whole structures analytically. In performing modal tests, it is important to simulate these matrices as boundary mass and stiffness. A procedure to find boundary mass and stiffness is shown, and a numerical example is given to show that the proposed method is effective for predicting accurate frequencies of whole structures.

Nomenclature

$[I]$	=	unit matrix
$[K]$	=	stiffness matrix
$[\bar{K}]$	=	reduced stiffness matrix
$[M]$	=	mass matrix
$[\bar{M}]$	=	reduced mass matrix
m	=	mass of component B
$[R]$	=	transformation matrix defined by Eq. (3)
$\{x\}$	=	elastic displacements
ΔK	=	boundary stiffness
ΔM	=	boundary mass
σ	=	frequency
Ω_i	=	angular frequency of structures
$\bar{\omega}_B$	=	boundary frequency of untested component
ω_i	=	angular frequency of components

Subscripts

A	=	component subjected to modal tests
B	=	untested components
b	=	boundary
i	=	internal
p	=	coordinate with boundary mass and stiffness
q	=	coordinates without boundary mass and stiffness

Introduction

SATELLITE communication systems have been used for providing various services and have received innovative technologies to improve communication quality. Large satellite antennas are one of the technologies to realize an economical system with high quality. Because they give high antenna gain and high pointing, portable terminals have become smaller and lower in price.

Presented as Paper 2004-1792 at the AIAA/ASME/ASCE/AHS/ASC 45th Structures, Structural Dynamics, and Materials Conference, Palm Springs, CA, 19–22 April 2004; received 30 April 2004; revision received 11 November 2004; accepted for publication 24 November 2004. Copyright © 2005 by the American Institute of Aeronautics and Astronautics, Inc. All rights reserved. Copies of this paper may be made for personal or internal use, on condition that the copier pay the \$10.00 per-copy fee to the Copyright Clearance Center, Inc., 222 Rosewood Drive, Danvers, MA 01923; include the code 0022-4650/05 \$10.00 in correspondence with the CCC.

*Professor, Department of Mechanical Engineering, 3-5-1 Johoku, Hamamatsu. Senior Member AIAA.

†Engineer, Amusement Rides Section, 1-13-18 Esaka-cho, Suita.

We have had problems to overcome, however, in developing large satellite antennas. The first problem is the setting of the antennas in the fairing envelope of launch vehicles. Deployable antennas can be a solution to this problem; therefore, they have been extensively studied.^{1–3} One of the other problems is the fulfillment of required performance on natural frequency.⁴ Frequency is an important design requirement to avoid coupling with a satellite in launch and control systems in orbit. We have to confirm antenna frequencies by modal tests even though the antennas have increased in size. However, it becomes increasingly difficult to perform modal tests for large deployed antennas because they are not strong enough to withstand the force caused by gravity. The focus of research on this problem is to verify the stiffness requirement without testing the whole structures. It is an effective method to divide a structure into several components and to predict the frequencies of the whole structure by using component modal test results. Component mode synthesis⁵ is a powerful analysis tool for frequency prediction in such a case. Fixed-constraint normal modes with a set of constraint modes, proposed by Craig and Bampton,⁶ enable the prediction of accurate frequencies. However, it is difficult to fix the boundaries of components in modal tests. The use of free-free normal modes eliminates the need for constraint modes. However, this results in solutions that are more susceptible to truncation error in higher modes. MacNeal⁷ proposed a method that accounts for the static contribution of neglected modes to minimize the truncation error. Although the MacNeal method is efficient, the method has not met with wide acceptance because of using impedance/admittance terminology. Rubin⁸ introduced residual inertia and dissipative effects to the MacNeal method. A method proposed by Karpel et al.⁹ is based on testing components with the interface coordinates loaded with rigid, heavy dummy masses supported by soft springs. Dummy masses generate local displacements near the boundaries to obtain dynamic properties of the whole structures. The low sensitivity of the method to the size of the boundary mass term allowed an easy design of the boundary mass with good handling and safety qualities. Soucy and Humar¹⁰ propose an approach to component mode synthesis in which the characteristics of individual components are determined experimentally through modal and static tests. This approach uses a combination of three different types of modes: rigid-support normal modes, residual flexibility attachment modes, and static constraint modes. This method gives a new approach that allows determination of the test-based characteristics by testing the components when they are attached to supports with arbitrary stiffness.

This paper proposes a method to predict the dynamic characteristics of large deployable antennas with component tests. In this method, to simulate the dynamic behavior of the antenna the simplest case is considered to confirm the feasibility for application to real structures. Namely, the reduced mass and stiffness matrices of untested components are replaced with a mass and a spring (boundary mass and stiffness) attached to the boundary. At first, theoretical formulation to find the boundary mass and stiffness is described. Next, we show that frequencies of the structure can be obtained analytically with reduced mass and stiffness matrices at boundary degrees of freedom. Finally, a numerical example is shown to demonstrate the effectiveness of the proposed method.

Formulation

Dynamic Equation of Tested Component

We considered a large deployable structure (antenna) consisting of several elastic components interconnected as shown in Fig. 1. Components are numbered with Arabic numerals. We define component A as the component subjected to modal tests, and the rest of the components (untested components) are called component B. In Fig. 1, component 4 is the tested component, and components 1, 2, and 3 are the untested components. Mass and stiffness matrices of component B are reduced to the boundary degrees of freedom because of considering the effect of component B in component modal tests. The dynamic analysis of component A with the reduced matrices at the boundary degrees of freedom gives frequencies of the structure as shown in a numerical example of this paper. Therefore, it is expected that we measure the dynamic characteristics of the structure by component modal tests if we determine the mass and stiffness properly attached to the boundary. It is impossible to determine unique boundary masses and springs from the reduced mass and stiffness matrices when we consider both translational and rotational degrees of freedom. Although the reduced matrices are effective in the mathematical approach, all of the elements of the matrices do not necessarily have physical meanings. Therefore, it is important how to simulate the mass and stiffness for accurate frequency verification. The proposed method in this paper considers the simplest case to confirm the feasibility for application to real structures. So, the reduced mass and stiffness matrices are replaced with a mass and a spring (boundary mass and stiffness) attached to the boundary, as shown in Fig. 2. The summary of theoretical formulation is described as follows.

The undamped, linear equation of motion for component B can be expressed as

$$-\omega_B^2 \begin{bmatrix} M_{B,ii} & M_{B,ib} \\ M_{B,bi} & M_{B,bb} \end{bmatrix} \begin{Bmatrix} x_{B,i} \\ x_{B,b} \end{Bmatrix} + \begin{bmatrix} K_{B,ii} & K_{B,ib} \\ K_{B,bi} & K_{B,bb} \end{bmatrix} \begin{Bmatrix} x_{B,i} \\ x_{B,b} \end{Bmatrix} = \{0\} \quad (1)$$

Solving Eq. (1) for $\{x_{B,i}\}$ in terms of $\{x_{B,b}\}$ gives the relationship

$$\{x_{B,i}\} = [R_B]\{x_{B,b}\} \quad (2)$$

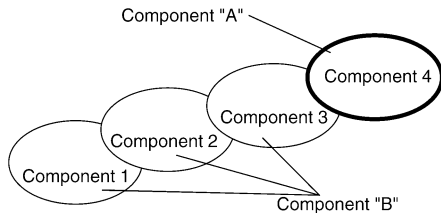


Fig. 1 Structure consisting of several components.

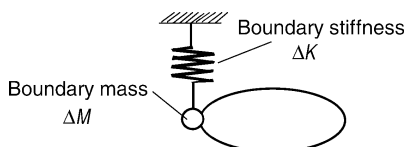


Fig. 2 Component A subjected to modal tests.

where

$$[R_B] = -([K_{B,ii}] - \sigma^2[M_{B,ii}])^{-1}([K_{B,ib}] - \sigma^2[M_{B,ib}]) \quad (3)$$

Equation (2) shows the relationship between internal displacement and boundary displacement when component B is vibrated. However, we must consider component B as part of the structure to measure the dynamic characteristics of the structure by component modal tests. This means that Eq. (2) holds when structure is vibrated. In other words, Eq. (2) is just an assumption that $[R_B]\{x_{B,b}\}$ is replaced with $\{x_{B,i}\}$ when frequency σ is not equal to structure frequency, and therefore $\{x_{B,i}\}$ does not give the internal displacement when the structure is vibrated. The effect of component B on dynamic characteristics obtained by component modal tests varies with frequency in Eq. (2). Therefore, we use an arbitrary frequency σ in place of frequency ω_B . We define the dynamic transformation matrix with respect to an arbitrary frequency σ . So, component displacements are expressed by

$$\begin{Bmatrix} x_{B,i} \\ x_{B,b} \end{Bmatrix} = \begin{bmatrix} R_B \\ I \end{bmatrix} \{x_{B,b}\} \quad (4)$$

Substituting Eq. (4) into Eq. (1) and premultiplying it by $[R_B^T I]$, we obtain the equation of motion for the boundary displacements as

$$-\bar{\omega}_B^2 [\bar{M}_B]\{x_{B,b}\} + [\bar{K}_B]\{x_{B,b}\} = \{0\} \quad (5)$$

where the reduced mass and stiffness matrices can be written as

$$\begin{aligned} [\bar{M}_B] &= \begin{bmatrix} R_B \\ I \end{bmatrix}^T \begin{bmatrix} M_{B,ii} & M_{B,ib} \\ M_{B,bi} & M_{B,bb} \end{bmatrix} \begin{bmatrix} R_B \\ I \end{bmatrix} \\ [\bar{K}_B] &= \begin{bmatrix} R_B \\ I \end{bmatrix}^T \begin{bmatrix} K_{B,ii} & K_{B,ib} \\ K_{B,bi} & K_{B,bb} \end{bmatrix} \begin{bmatrix} R_B \\ I \end{bmatrix} \end{aligned} \quad (6)$$

The solution of the reduced equation (5), called boundary frequency $\bar{\omega}_B$, is not equal to that of the original Eq. (1). Therefore, we intentionally use $\bar{\omega}_B$ as solution of Eq. (5) to address the difference from frequency ω_B of Eq. (1). It can be seen that the reduced mass and stiffness matrices depend on the value of frequency σ . There is no error in these matrices only when frequency σ is equal to an antenna frequency. Adding the reduced mass and stiffness matrices to the boundary of component A, the dynamic equation of tested component is expressed by

$$-\Omega^2 [\hat{M}_A]\{\hat{x}_A\} + [\hat{K}_A]\{\hat{x}_A\} = \{0\} \quad (7)$$

where

$$\begin{aligned} [\hat{M}_A] &= \begin{bmatrix} M_{A,ii} & M_{A,ib} \\ M_{A,bi} & M_{A,bb} + \bar{M}_B \end{bmatrix} \\ [\hat{K}_A] &= \begin{bmatrix} K_{A,ii} & K_{A,ib} \\ K_{A,bi} & K_{A,bb} + \bar{K}_B \end{bmatrix} \\ \{\hat{x}_A\} &= \begin{Bmatrix} \hat{x}_{A,i} \\ \hat{x}_{A,b} \end{Bmatrix} \end{aligned} \quad (8)$$

Boundary Mass and Stiffness

We partition displacements $\{\hat{x}_A\}$ in Eq. (7) into two groups: one translational displacement at a boundary node $\{\hat{x}_{A,p}\}$ and the rest $\{\hat{x}_{A,q}\}$. By partitioning mass and stiffness matrices corresponding to $\{\hat{x}_{A,p}\}$ and $\{\hat{x}_{A,q}\}$, Eq. (7) is rewritten as

$$-\Omega^2 \begin{bmatrix} \hat{M}_{A,pp} & \hat{M}_{A,pq} \\ \hat{M}_{A,qp} & \hat{M}_{A,qq} \end{bmatrix} \begin{Bmatrix} \hat{x}_{A,p} \\ \hat{x}_{A,q} \end{Bmatrix} + \begin{bmatrix} \hat{K}_{A,pp} & \hat{K}_{A,pq} \\ \hat{K}_{A,qp} & \hat{K}_{A,qq} \end{bmatrix} \begin{Bmatrix} \hat{x}_{A,p} \\ \hat{x}_{A,q} \end{Bmatrix} = \{0\} \quad (9)$$

Similarly, the dynamic equation of component A is expressed as

$$-\omega_A^2 \begin{bmatrix} M_{A,pp} & M_{A,pq} \\ M_{A,qp} & M_{A,qq} \end{bmatrix} \begin{Bmatrix} x_{A,p} \\ x_{A,q} \end{Bmatrix} + \begin{bmatrix} K_{A,pp} & K_{A,pq} \\ K_{A,qp} & K_{A,qq} \end{bmatrix} \begin{Bmatrix} x_{A,p} \\ x_{A,q} \end{Bmatrix} = \{0\} \quad (10)$$

Equations (9) and (10) can be reduced to $\{\hat{x}_{A,p}\}$ and $\{x_{A,p}\}$ as

$$-\Omega^2 [\hat{M}'_A] \{\hat{x}_{A,p}\} + [\hat{K}'_A] \{\hat{x}_{A,p}\} = \{0\} \quad (11)$$

$$-\omega_A^2 [M'_A] \{x_{A,p}\} + [K'_A] \{x_{A,p}\} = \{0\} \quad (12)$$

Because this method limits the number of boundary mass and stiffness to one for each boundary node, $[\hat{M}'_A]$ and $[M'_A]$ are not a matrix but scalar. Therefore, the difference between $[\hat{M}'_A]$ and $[M'_A]$ means the boundary mass. For structures with several boundary nodes, boundary mass for each boundary node is found by using Eqs. (11) and (12), and we divide these masses by the number of boundary nodes. Then we treat obtained masses as boundary mass attached to boundaries. Boundary stiffness is also found in a similar way. As stated before, the effect of component B on dynamic characteristics obtained by component modal tests varies with frequency σ . Therefore, the boundary mass and stiffness are selected for an individual frequency. Namely, we must select them so that a desired frequency of the structure is obtained by component modal testing.

Numerical Example

Analytical Model

A numerical example is given to demonstrate the effectiveness of the proposed method. The method was applied to a cantilever beam as indicated in Fig. 3. The beam, made of carbon fiber reinforced plastics, consists of two components. For simplicity, only in-plane (x - y plane) bending modes were considered. Figure 4 shows test configurations of component A with boundary mass ΔM and stiffness ΔK . For example, in testing component 1, we use boundary mass and stiffness found by reducing mass and stiffness matrices of component 2. Boundary stiffness is created by wire (and spring if required) suspending the tested component.

Frequencies of Component A with the Reduced Mass and Stiffness Matrices

We calculated frequencies of component A with the reduced mass and stiffness matrices of component B at boundary degrees of free-

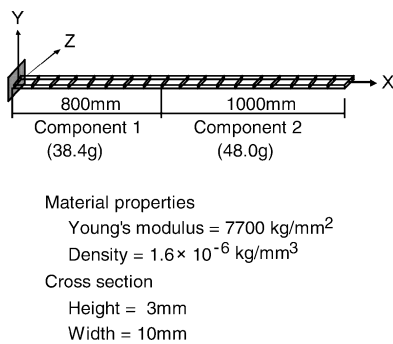


Fig. 3 Cantilever beam.

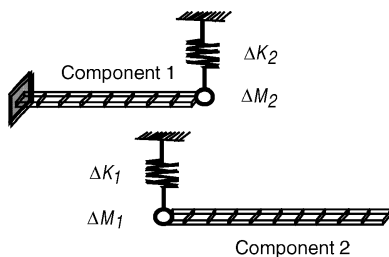


Fig. 4 Test configuration of component A with boundary mass and stiffness.

Table 1 Calculated frequencies of component A with reduced mass and stiffness matrices

Component A	Mode no.	Beam frequencies used in finding boundary mass and stiffness, Hz			
		1.0	6.4	17.9	35.0
1	1	1.0	6.4	13.6	14.9
	2	9.3	14.6	17.9	35.0
	3	40.4	42.8	51.1	63.4
	4	98.8	100.5	111.4	121.3
2	1	1.0	1.0	1.4	1.8
	2	6.4	6.4	7.6	11.9
	3	18.9	18.7	17.9	35.0
	4	42.4	42.1	40.1	38.6

Table 2 Boundary mass and stiffness of component B

Mode no.	Component 1		Component 2	
	ΔM_1 , g	ΔK_1 , N/mm	ΔM_2 , g	ΔK_2 , N/mm
1	278.3	1.78E0	275.3	1.17E1
2	33.0	5.85E1	27.2	6.59E1
3	176.0	2.42E3	184.1	2.23E3
4	58.2	2.88E3	52.1	2.84E3

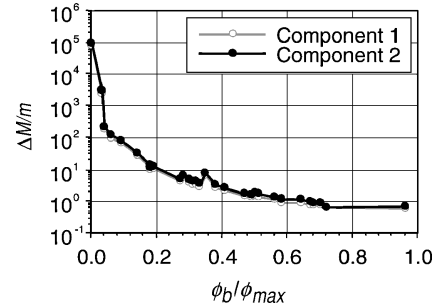


Fig. 5 Variation in boundary mass.

dom. Table 1 lists calculated frequencies. Beam frequencies are found by finite element analysis. In this case, those frequencies are considered as exact frequencies. Frequencies of 1.0, 9.3, 40.4, and 98.8 Hz are obtained in using the beams' first frequency as frequency σ to calculate boundary mass and stiffness when component 1 is tested. The first beam frequency of 1.0 Hz is obtained. The second and higher frequencies of the beam also are obtained. When component 2 is tested, the beam frequencies of 1.0, 6.4, 17.9, and 35.0 Hz are calculated. This shows that we obtain beam frequencies by adding the reduced mass and stiffness matrices of component B at the boundary degrees of freedom. This means that the proposed method gives useful information to determine which frequency corresponds to the beam frequency. As shown in Table 1, we can obtain beam frequency even if component A is component 1 or component 2. It is reasonable that we consider identical frequencies obtained by both tests of components 1 and 2 beam frequencies.

Boundary Mass and Stiffness

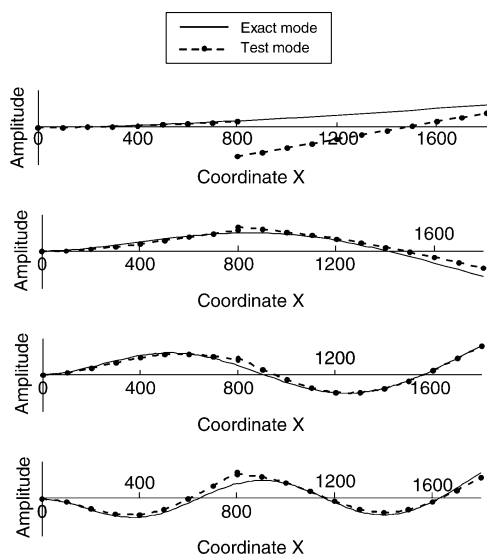
Boundary mass and stiffness are listed in Table 2. This table shows that boundary mass in the first and third mode is larger than that in the second and fourth modes. The cause of the tendency depends on the amplitude of the boundary node. Figure 5 shows variation in 36 boundary masses. The longitudinal axis is boundary mass normalized by a mass of component B. The lateral axis shows the amplitude of the boundary node normalized by the maximum amplitude of each beam mode. It can be seen that boundary mass reduces as the amplitude of the boundary node increases. This shows that it is desirable to select boundary nodes so that their displacements become large to obtain smaller boundary mass. Because large deployable antennas consist of several components, we select such boundary nodes by

Table 3 Measured frequencies with boundary mass and stiffness

Component A	Mode no.	Beam frequencies used in finding boundary mass and stiffness, Hz			
		1.0	6.4	17.9	35.0
1	1	1.0	6.4	17.9	22.0
	2	22.8	24.1	23.4	35.0
	3	73.4	74.8	73.6	74.4
	4	153.2	154.6	153.3	154.0
2	1	0.0	0.0	0.0	0.0
	2	1.0	6.4	14.0	11.9
	3	14.6	16.2	17.9	35.0
	4	47.0	48.4	47.1	48.6
Beam	—	1.0	6.4	17.9	35.0

Table 4 MAC

Mode no.	Component 1	Component 2
1	1.00	0.96
2	0.99	0.89
3	0.97	0.96
4	0.85	0.93

**Fig. 6** Beam modes and measured component modes.

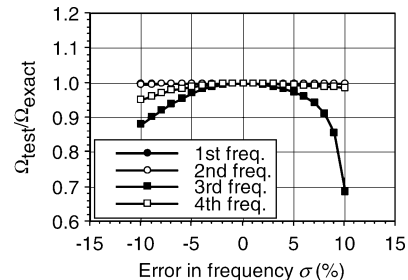
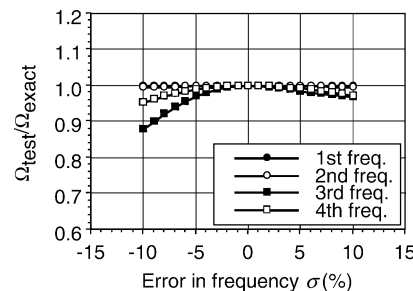
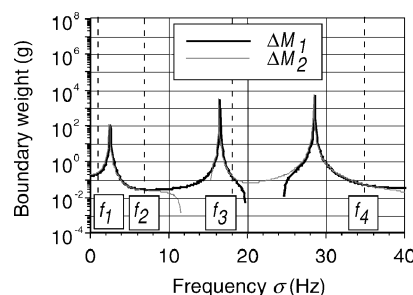
changing the tested component. Light boundary mass is significantly important to perform modal tests of large flexible structures.

Simulated Test Results

The simulated test models are constructed by using finite element models of tested component with a boundary mass and a boundary spring. In this paper, we consider analytical results to be modal test.

Table 3 lists the frequencies obtained from component modal tests. By testing component 1, frequencies of 1.0, 22.8, 73.4, and 153.2 Hz were obtained when the first beam frequency is used as frequency σ to calculate the boundary mass and stiffness. It can be seen that the test of component 1 can provide the first beam frequency of 1.0 Hz. For the second and higher frequencies, beam frequencies are obtained by component 1 modal tests. Table 3 also shows that we can obtain frequencies identical to beam frequencies by component 2 modal tests.

Figure 6 shows the lower four modes of the beam. The solid line shows the exact mode of the beam, and the dotted line indicates the measured component mode obtained by modal tests. We check the correspondence between these modes for components 1 and 2. The modal assurance criteria (MAC) are used to check the modal correspondence. The results are listed in Table 4. Both modes are almost identical. There is discontinuity at the boundary especially for the first mode. This is why components 1 and 2 are subjected to modal tests separately. Because it is important to show that test mode

**Fig. 7** Beam frequency error in modal tests of component 1.**Fig. 8** Beam frequency error in modal tests of component 2.**Fig. 9** Variation in boundary mass.

corresponds to analytical mode, we do not make the displacements equal at the boundary node. The proposed method is effective in obtaining the dynamic characteristics of the beam and has the potential to verify the frequency requirement of large space structures.

Effect of Error in Frequency σ

Figures 7 and 8 indicate a variation in the accuracy of the measured frequencies as a result of the error of frequency σ used in finding the boundary mass and stiffness of component B. It can be seen that there is no error in measured frequencies when frequency σ is exact. Even if frequency σ has errors, the frequency error has little influence on the measured first and second frequencies. In these cases, the proposed method is effective to obtain accurate beam frequencies. On the other hand, the accuracy of the third frequency decreases by 30% for a frequency error σ of 10%. We obtain different frequencies from tests of components 1 and 2 when the error in frequency σ is 10%. Therefore, we do not consider these frequencies to be the beam frequency. However, component tests give almost identical frequencies when the error in frequency σ is -10% . As one does not know the beam frequency, we consider the measured frequency the beam frequency although the measured frequency is not accurate. However, even in such a case the proposed method has a possibility to improve the frequency error by changing the division of the structure into components. This can be explained by the relationship between frequency σ and boundary mass or boundary stiffness. Figure 9 shows variation in boundary mass when frequency σ increases from 0 to 40 Hz. Dotted lines show the lower four beam frequencies. Boundary mass variations are small for the first, second, and fourth frequencies. However, boundary masses change drastically near the third beam frequency. This is why the third frequency error increases as just mentioned. Figure 10 shows

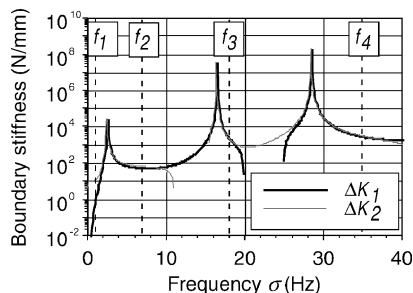


Fig. 10 Variation in boundary stiffness.

variation in boundary stiffness. Variation in boundary stiffness has the same tendency as that in boundary mass. Boundary stiffness in the third frequency also has a large change to small increment of frequency σ . It is effective to divide the beam (structure) into several components so that both changes in boundary mass and stiffness are small for improving third frequency accuracy.

Conclusions

This paper proposes a method to predict the dynamic characteristics of large satellite antennas with component tests. Space structures (satellite antennas) are divided into several components. The effect of untested components is considered as mass and stiffness attached to the boundary of a component subjected to modal testing. The following conclusions were obtained:

- 1) The procedure to find boundary mass and stiffness is clarified.
- 2) Boundary mass depends on the amplitude of a boundary. It is effective to select boundary nodes so that their displacements become larger to obtain smaller boundary masses.

3) A method determines which measured frequency corresponds to the frequency of the whole structure.

4) A numerical example shows that the proposed has the potential to verify the frequency requirement of large space structures.

References

- ¹Misawa, M., Kumazawa, H., and Minomo, M., "Configuration and Performance of 30/20 GHz Band Shaped-Beam Antenna for Satellite Use," AIAA Paper 84-0868, May 1984.
- ²Johnston, W. A., Jr., "ATS-6 Experimental Communications Satellite-Report on Early Orbital Results," *Journal of Spacecraft and Rockets*, Vol. 13, No. 2, 1976, pp. 91–98.
- ³Craig, A. R., and Warren L. S., "Large Deployable Antenna Program," NASA CR-4410, Oct. 1991.
- ⁴Misawa, M., "Stiffness Design of Deployable Satellite Antennas in Deployed Configuration," *Journal of Spacecraft and Rockets*, Vol. 35, No. 3, 1998, pp. 380–386.
- ⁵Craig, R. R., Jr., "Coupling of Substructures for Dynamic Analyses: An Overview," AIAA Paper 2000-1573, April 2000.
- ⁶Craig, R. R., Jr., and Bampton, M. C. C., "Coupling of Substructures for Dynamic Analyses," *AIAA Journal*, Vol. 6, No. 7, 1968, pp. 1313–1319.
- ⁷MacNeal, R. H., "A Hybrid Method of Component Mode Synthesis," *Computers and Structures*, Vol. 1, No. 4, 1971, pp. 581–601.
- ⁸Rubin, S., "Improved Component-Mode Representation for Structural Dynamic Analysis," *AIAA Journal*, Vol. 13, No. 8, 1975, pp. 995–1006.
- ⁹Karpel, M., Raveh, D., and Ricci, S., "Ground Modal Tests of Space-Structure Component Using Boundary Masses," *Journal of Spacecraft and Rockets*, Vol. 33, No. 2, 1996, pp. 272–277.
- ¹⁰Soucy, Y., and Humar, J. L., "Experimental Verification of a Test-Based Hybrid Component Mode Synthesis Approach," *AIAA Journal*, Vol. 41, No. 5, 2003, pp. 912–923.

L. Peterson
Associate Editor